Standard Gibbs energy of metabolic reactions: VI. Glyceraldehyde 3-phosphate dehydrogenase reaction

In honor of Stanley I. Sandler for his great contributions to our scientific community.

Thorsten Greinert,[a] Kristina Vogel,[b] Jan-Kristof Mühlenweg,[a] Gabriele Sadowski,[a] Thomas Maskow,[b] Christoph Held[a]*

[a] Laboratory of Thermodynamics, Department of Biochemical and Chemical Engineering, Technische Universitaet Dortmund, Emil-Figge-Str. 70, 44227 Dortmund, Germany

[b] UFZ - Helmholtz Centre for Environmental Research, Dept. Environmental Microbiology, Leipzig, Permoserstr. 15, D-04318 Leipzig, Germany

Keywords:

Thermodynamics; activity coefficients; equilibrium constant; enthalpy of reaction; ePC-SAFT; calorimetry

* corresponding author: christoph.held@tu-dortmund.de

Symbols

Greek letters

Symbol	Property	Unit
$\varepsilon^{A_iB_i}/k_B$	association-energy parameter	K
γ_i^m	generic activity coefficient of component i on molality-base	(kg water) mol^{-1}
$\gamma_i^{*,m}$	rational activity coefficient of component i on molality-base	-
$\gamma_i^{\infty,m}$	generic activity coefficient of component i at infinite dilution on molality-base	(kg water) mol^{-1}
κ^{AiBi}	association-volume parameter	-
ρ	density	kg m^{-3}
σ_i	segment diameter of component i	Å
ϕ	osmotic coefficient	-
ν_i	stoichiometric coefficient of component i	-

Latin letters

Symbol	Property	Unit
a_i	activity of component i	-
A	absorbance	-
A^{res}	residual Helmholtz energy	J

A^{hc}	hard-chain contribution to Helmholtz energy	J
A^{disp}	dispersion contribution to Helmholtz energy	J
A^{assoc}	association contribution to Helmholtz energy	J
A^{ion}	ionic contribution to Helmholtz energy	J
$\Delta^R g'^0$	standard Gibbs energy of biochemical reaction	J mol^{-1}
$\Delta^R g'^{0,obs}$	observed standard Gibbs energy of biochemical reaction	J mol^{-1}
$\Delta^R h'^0$	standard enthalpy of biochemical reaction	J mol^{-1}
$\Delta^R h'^{0,obs}$	observed standard enthalpy of biochemical reaction	J mol^{-1}
k_B	Boltzmann constant ($1.38 \cdot 10^{-23} \cdot m^2 \cdot kg \cdot s^{-2} \cdot K^{-1}$)	J K^{-1}
k_{ij}	binary interaction parameter of components i and j	-
K'_a	thermodynamic equilibrium constant of biochemical reaction	-
K'_γ	activity-coefficient ratio of biochemical reaction	-
K'_m	equilibrium-molality ratio of biochemical reaction	-
m_i	molality of component i	mol $(kg\ water)^{-1}$
m_i^{seg}	segment number of component i	-
M_i	molar mass of component i	g mol^{-1}
N_i^{assoc}	number of association sites of component i	-
pK_A	$-\log_{10}$ of acid dissociation constant	-
R	ideal gas constant (8.314 J mol^{-1} K^{-1})	J mol^{-1} K^{-1}

T	temperature	K
u_i/k_B	dispersion-energy parameter of component i	K
w	weighing factor	-
z	valence of an ion	-

24

Abstract

Glycolysis is a very central metabolic pathway for many organisms because it represents a key component in their energy production. For this reason, it has always been an extensively studied pathway. The glyceraldehyde 3-phosphate dehydrogenase (GDH) reaction is an important reaction of glycolysis yielding nicotinamide adenine dinucleotide (NADH). The aim of this work is to investigate the thermodynamics of the GDH reaction and determine the standard Gibbs energy of reaction $\Delta^R g'^0$ and standard enthalpy of reaction $\Delta^R h'^0$. Currently, so-called 'standard' data exist in the literature that depend on the conditions they were measured at. In this work, a $\Delta^R g'^0$ and $\Delta^R h'^0$ values were determined that are independent from reaction conditions by accounting for the activity coefficients of the reacting substances. Therefore, the equation of state electrolyte Perturbed-Chain Statistical Associating Fluid Theory (ePC-SAFT) was used. The required ePC-SAFT parameters were taken from literature or fitted to new experimental osmotic coefficients. A value of $\Delta^R g'^0$ = 51.5±0.4 kJ mol^{-1} was determined at 298.15 K. This value deviates by up to 10 kJ mol^{-1} from existing literature values, caused by activity coefficients in the reaction medium. It can be used to determine the Gibbs energy of reaction $\Delta^R g'$, which will allow statements concerning the feasibility of the GDH reaction. Further, a method is presented to predict influences of pH, initial substrate concentration and Mg^{2+} concentration on the reaction equilibrium. Finally, we measured the standard reaction enthalpy for the GDH reaction $\Delta^R h'^0$ by titration calorimetric measurements ($\Delta^R h'^0$ = 4.6±0.1 kJ mol^{-1}). This value was within van 't Hoff evaluated $\Delta^R h'^0$ (9±16 kJ mol^{-1}) using temperature-dependent equilibrium constants from equilibrium measurements corrected by ePC-SAFT predicted activity coefficients.

Introduction

Glycolysis plays an important role in the assimilation of sugars of many organisms because of the oxidation of glucose to pyruvate, adenosine triphosphate and β-nicotinamide adenine dinucleotide (NADH) in a cell. This raises the need for understanding glycolysis in more detail, and already a large amount of literature is related to glycolysis pathway *(1–6)*. Furthermore, also thermodynamics of glycolysis has been investigated in order to gain deeper understanding. However, this led to misinterpretations of the feasibility of the pathway, because positive values of Gibbs energy of reaction $\Delta^R g'$ were calculated in cells, which means that glycolysis is thermodynamically unfeasible *(7–10)*. $\Delta^R g'$ requires the standard Gibbs energy of reaction $\Delta^R g'^0$, which reflects the ratio of the metabolite activities at equilibrium. $\Delta^R g'^0$ was identified to be a possible source of the misinterpretation of the found $\Delta^R g'$ values at cellular conditions. Further, accounting for activity coefficients for the consistent determination of $\Delta^R g'^0$ is recommended *(11–17)*. Thus, in previous works new $\Delta^R g'^0$ values were generated for several glycolytic reactions in order to rectify the thermodynamic description of glycolytic reactions *(11–17)*.

The present work focuses on determining an activity-based $\Delta^R g'^0$ value for the glyceraldehyde 3-phosphate dehydrogenase (GDH) reaction. GDH is the first reaction of the pay-off phase of glycolysis, which is connected to a production of ATP and NADH. Besides the production of NADH and the resulting importance of this reaction, the GDH reaction furthermore represents a crucial bottleneck for glycolysis *(7)* meaning that a correct thermodynamic interpretation of glycolysis strongly depends on the fundamental understanding of this reaction. Thus, the concentration-based observed $\Delta^R g'^{0,obs}$ values available from literature, which differ by up to 5 kJ mol^{-1} from each other for the GDH reaction *(7,18–21)*, will be compared to a new activity-based value from this work in order to find a reliable $\Delta^R g'^0$ for the usage in any future work that

is connected to this reaction. Different procedures yield activity-based values, for instance Alberty calculated standard Gibbs energies of reaction for other reactions including NADH or nicotinamide adenine dinucleotide phosphate from standard Gibbs energies of formation *(22,23)*. In this work, in vitro measurements are performed investigating influences of i) the initial substrate concentration, ii) temperature, iii) pH and iv) Mg^{2+} concentration on the reaction equilibrium. These measurements were combined with activity coefficients determined with an equation of state, the electrolyte Perturbed-Chain Statistical Associating Fluid Theory (ePC-SAFT) *(24,25)* yielding an activity-based $\Delta^R g'^0$ value for the GDH reaction. ePC-SAFT allows to reliably predict activity coefficients of substances in multi-component systems with high accuracy describing interactions between charged (bio-)molecules *(26–29)*. This is required to explain effects of the reaction conditions on the equilibrium and kinetics of biochemical reactions *(27–37)*.

Thermodynamic Formalism for Glyceraldehyde 3-phosphate Dehydrogenase Reaction

In the GDH reaction, D-glyceraldehyde 3-phosphate (GAP), nicotinamide adenine dinucleotide (NAD^+) and inorganic phosphate (P_i) are converted to 1,3-bisphospho-D-glycerate (BPG) and the reduced form of NADH with a proton. The biochemical expression is given in eq. (1), while the species shown in eq. (2) are considered for the classical chemical expression.

$$GAP + NAD^+ + P_i \rightleftharpoons BPG + NADH + H^+ \quad (1)$$

$$GAP^{2-} + (NAD^+)^- + HPO_4^{2-} \rightleftharpoons BPG^{4-} + NADH^{2-} + H^+ \quad (2)$$

In this work, all investigations are based on eq. (1). The Gibbs energy of reaction $\Delta^R g'$ explains whether or not a single (bio-)chemical reaction occurs under prevailing reaction conditions.

Negative values indicate that reactions are thermodynamically feasible, while others with positive values are not. $\Delta^R g'$ is calculated from the standard Gibbs energy of reaction $\Delta^R g'^0$, see eq. (3).

$$\Delta^R g' = \Delta^{\mathrm{R}} \mathrm{g}'^0 + \mathrm{RT} \ln\left(\prod_i a_i^{\nu_i}\right) \tag{3}$$

To calculate the standard Gibbs energy of reaction $\Delta^R g'^0$, the thermodynamic equilibrium constant K'_a and eq. (4) are used. K'_a is calculated from the molality-ratio at equilibrium K'_m and the activity-coefficient ratio at equilibrium K'_γ according to eq. (5).

$$\Delta^R g'^0 = -RTln(K'_a) \tag{4}$$

$$K'_a = K'_m \cdot K'_\gamma \tag{5}$$

K'_m is defined as seen in eq. (6), based on the sum of species molalities at equilibrium. K'_γ is based on rational activity coefficients and is calculated with eq. (7). According to eq. (1), all properties of a component are species-averaged, including activity coefficients.

$$K'_m = \frac{m^{eq}_{\mathrm{BPG}} \cdot m^{eq}_{\mathrm{NADH}} \cdot m^{eq}_{\mathrm{H^+}}}{m^{eq}_{\mathrm{GAP}} \cdot m^{eq}_{NAD^+} \cdot m^{eq}_{\mathrm{P_i}}} \tag{6}$$

$$\mathrm{K'_\gamma} = \frac{\gamma^{*,m,eq}_{\mathrm{BPG}} \cdot \gamma^{*,m,eq}_{\mathrm{NADH}} \cdot \gamma^{*,m,eq}_{\mathrm{H^+}}}{\gamma^{*,m,eq}_{\mathrm{GAP}} \cdot \gamma^{*,m,eq}_{NAD^+} \cdot \gamma^{*,m,eq}_{\mathrm{P_i}}} \tag{7}$$

The rational activity coefficients with standard state '*hypothetical ideal solution*' $\gamma_i^{*,m}$ are calculated from the generic activity coefficients with standard state '*pure substance*' at present conditions γ_i^m and at infinite dilution $\gamma_i^{\infty,\mathrm{m}}$.

$$\gamma_i^{*,m} = \frac{\gamma_i^m}{\gamma_i^{\infty,\mathrm{m}}} \tag{8}$$

In this work, '*hypothetical ideal solution*' is defined as a solution of 1 mol kg^{-1} of the substance diluted in water and an activity coefficient equal to the activity coefficient of the substance infinitely diluted in water, meaning $\gamma_i^{*,m} = 1$.

The standard enthalpy of reaction $\Delta^R h'^0$, which describes the temperature dependence of the thermodynamic equilibrium constant K'_a, can be calculated with the van 't Hoff equation, see eq. (9).

$$\left(\frac{dlnK'_a}{dT}\right)_p = \frac{\Delta^R h'^0}{RT^2} \tag{9}$$

Assuming a temperature-independent $\Delta^R h'^0$, the integration of eq. (9) yields eq. (10) which allows to calculate $\Delta^R h'^0$ from at least two K'_a values and $K'_a(T_2)$ if $\Delta^R h'^0$ and $K'_a(T_1)$ are known.

$$ln\left(\frac{K'_a(T_2)}{K'_a(T_1)}\right) = -\frac{\Delta^R h'^0}{R}\left(\frac{1}{T_2} - \frac{1}{T_1}\right) \tag{10}$$

Materials and Methods

Materials

All substances used in this work are listed in Table S1 and have been used without further purification. The substrate GAP had to be synthesized from its diethyl acetal barium salt, as described in the Supporting Information. In this work, the lyophilized form of GDH received from rabbit muscle was used without further modifications or purifications (Enzyme Commission number 1.2.1.12). The supplier tested the composition with the result of 100% of protein (Biuret). Its enzymatic activity for relevant reactions was tested by the supplier with results of 0.01% for 3-phosphoglyceric phosphokinase reaction, 0.0% for triosephosphate isomerase reaction, 0.00% for lactic dehydrogenase reaction, 0.01% for myokinase reaction and 0.00% for pyruvate kinase

reaction. This is important, as reactions occurring simultaneously to the GDH reaction would influence the equilibrium measurements. The water used in this work was freshly prepared ultra-pure water from a Millipore® purification system (Merck KGaA, Darmstadt, Germany). The substances NAD^+ and its reduced form NADH were provided as hydrates, thus, the water content provided by the supplier was considered in all calculations. The water contents were 5% by mass for both. All solutions were composed by weight with an analytical balance XS205 (Mettler Toledo GmbH, Gießen, Germany) with an accuracy of 0.01 mg.

Equilibrium Experiments

The equilibrium experiments were carried out in 5 mL Eppendorf Tubes® (Eppendorf AG, Hamburg, Germany), which were maintained at constant temperature and stirred by a ThermoMixer C (Eppendorf AG, Hamburg, Germany). Additionally, some samples were placed in an UV spectrometer SPECORD® 210 PLUS (Analytik Jena AG, Jena, Germany) using High Precision cuvettes (Hellma Analytics, Müllheim, Germany) with a pathway of 10 mm. Prior to the experiments, substrate solutions were freshly prepared. A buffer solution, which in this case is also a substrate solution, was prepared from monobasic and dibasic potassium phosphate solutions of the same molality, such that the desired pH was reached. This was ensured by pH measurement with a QpH 70 (VWR International GmbH, Darmstadt, Germany). A buffer concentration of 80 mmol kg^{-1} allowed to comfortably adjust the solution such that the desired pH was reached at the reaction equilibrium. Further, a substrate solution containing NADH was prepared with water. The enzyme glyceraldehyde 3-phosphate dehydrogenase was diluted in water. Afterwards, the substrate solutions were mixed such that the desired reaction conditions were achieved. If required, the pH was again adjusted to the desired value by adding potassium hydroxide solution to the reaction medium. Then, the enzyme solution was added, which initiated the reaction. The desired reaction temperature (298.15 K, 305.15 K or 310.15 K) was maintained by the ThermoMixer C or

the UV spectrometer within 0.1 K. When the concentration analysis showed that the NADH concentration did not change any further equilibrium was assumed to be reached; this was validated additionally by adding new substrate to the solution, yielding again a new equilibrium position. In particular, it was taken care that the enzyme was still active and converts the new substrate yielding a new NADH concentration.

Concentration Analysis

Prior to measurements of equilibrium concentrations in the UV spectrometer, a calibration curve of the UV absorption of NADH at 340 nm was determined for molalities between 0.1 and 0.7 mmol kg^{-1} NADH at different reaction conditions. The coefficient of determination of the linear calibration curves, consisting of six three-fold determinations, was >0.99. The molal extinction coefficient of NADH in 80 mmol kg^{-1} potassium phosphate buffer resulting from the linear calibration curve was 3698 kg mol^{-1} cm^{-1}. The proton activity at equilibrium was determined via pH measurements. It has to be noted, that these measurements yield the hydrogen activity $a_{H^+}^{eq}$ with the standard state '*hypothetical ideal solution*' as defined in this work because of the measurement method *(38)*. Given that no side reactions take place, the equilibrium molality of BPG m_{BPG}^{eq} is equal to the molality of NADH at equilibrium m_{NADH}^{eq}. The equilibrium molalities of NAD^+ $m_{NAD^+}^{eq}$, GAP m_{GAP}^{eq} and P_i $m_{P_i}^{eq}$ were calculated according to eqs. (11)-(13) from their initial molalities prior to the reaction $m_{\mathrm{i}}^{t=0}$ and from the equilibrium molality of NADH m_{NADH}^{eq}. Again under the assumption of no side reactions, these equations are correct as the substrates NAD^+, GAP and P_i are converted stoichiometrically such that the produced NADH equals the consumed substrates, respectively.

$$m_{NAD^+}^{eq} = m_{\mathrm{NADH}}^{t=0} - m_{\mathrm{NADH}}^{eq} \tag{11}$$

$$m_{GAP}^{eq} = m_{\mathrm{GAP}}^{t=0} - m_{\mathrm{NADH}}^{eq} \quad (12)$$

$$m_{P_i}^{eq} = m_{P_i}^{t=0} - m_{\mathrm{NADH}}^{eq} \quad (13)$$

To sum up, only the NADH concentrations and the pH value at equilibrium were experimentally measured, while the equilibrium concentrations of all other reacting substances were calculated from the above-mentioned equations (11)-(13). To give an estimation of the accuracy of the values provided in this work, we performed an error estimation by means of a Taylor series.

Titration calorimetric determination of $\Delta^R h'$

Two solutions were prepared for the calorimetric determination of $\Delta^R h'$. The GDH solution contained 0.83 µmol kg^{-1} GDH (97 U mg^{-1}), 400 mmol kg^{-1} potassium phosphate buffer pH 7 and 5 mmol kg^{-1} NAD$^+$. The GAP solution consisted of 5 mmol kg^{-1} GAP (53 mg ml^{-1} from Sigma Aldrich), 400 mmol kg^{-1} potassium phosphate buffer pH 7 and 5 mmol kg^{-1} NAD$^+$. A concentration of 400 mmol kg^{-1} potassium phosphate buffer was used to ensure a constant pH of 7 throughout the monitoring of the reaction heat from the beginning of the reaction to equilibrium. The calorimeter was a MicroCal PEAQ ITC (Malvern Panalytical GmbH, Kassel, Germany). Single injection measurements were performed, with GAP solution in the titration syringe and GDH solution in the sample cell. The reference cell was filled with water. The setup of the PEAQ-ITC was set to high feedback, reference power of 41.9 µW, stirrer speed of 750 rpm, titration speed of 0.5 µL s^{-1} and baseline recording of 150 s. Two injections were done. The first one with 0.4 µL and a spacing time of 300 s and the second with 35 µL and 3450 s spacing time. The first injection was ignored due to heat of dilution effects. The signal was recorded until it reached the baseline again, which occurred fast after about 8 minutes (see Fig. S2). The reference measurements were done with buffer in the titration syringe and GDH solution in the sample cell and GAP in the titration syringe and buffer in the sample cell to delete the heat of dilution. The reference signals

were then subtracted from the signal of the reaction. We performed the GDH reaction with substrate molalities of $m_{\mathrm{GAP}}^{t=0}$ = 0.9 mmol kg^{-1} and $m_{\mathrm{NAD+}}^{t=0}$ = 5 mmol kg^{-1} in 400 mmol kg^{-1} potassium phosphate buffer at pH 7.0 and 310.15 K.

Thermodynamic Modeling

The activity coefficients of the reacting substances, which are required to determine the thermodynamic equilibrium constant K_a' with eqs. (5) and (7) were predicted with the equation of state ePC-SAFT in this work. ePC-SAFT, as proposed by Held et al. *(24)*, is based on the original PC-SAFT version from Gross and Sadowski *(25)*, and it represents a revised version from original ePC-SAFT developed by Cameretti et al. *(39)*. Using ePC-SAFT instead of PC-SAFT was necessary in order to consider interactions involving anions and cations present in the reaction solution, which plays an important role for this reaction. Please note that a newer version of ePC-SAFT exists where the dependency of the dielectric constant on the reaction medium is considered *(40)*. In this work, all substances are highly diluted in water, meaning that the version falls back to original ePC-SAFT, where the dielectric constant of water is used. The prediction of thermodynamic properties such as activity coefficients within ePC-SAFT is based on the calculation of the residual Helmholtz energy A^{res} from four contributions, see eq. (14).

$$A^{res} = A^{hc} + A^{disp} + A^{assoc} + A^{ion} \tag{14}$$

A^{hc} is the Helmholtz energy of the reference fluid given by the hard-chain fluid which is calculated assuming a reference system of a hard chain which itself is composed of hard spheres. The other three contributions account for perturbations to this hard-chain reference fluid. A^{disp} includes molecular dispersive interactions, related to the van der Waals energy. A^{assoc} includes associative interactions, related to the hydrogen bonding forces and A^{ion} includes ionic interactions, described by a Debye-Hückel expression. Accounting for these contributions within ePC-SAFT requires five

pure-component parameters. The volume of the hard chains is described by the segment number m_i^{seg} and the segment diameter σ_i. The dispersive interactions are described by the dispersion-energy parameter u_i/k_B including the Boltzmann constant k_B. The hydrogen bonding interactions are described by the association-energy parameter $\varepsilon^{A_iB_i}/k_B$ and the association-volume parameter $\kappa^{A_iB_i}$. Additionally, the number of association sites N_i^{assoc} is required. Mixing rules, which are applied when calculating mixtures, are described in the Supporting Information (eqs. S1-S4).

Estimation of ePC-SAFT Parameters

The ePC-SAFT pure-component parameters for water, the ions H_3O^+, K^+, Mg^{2+} and Cl^-, for the buffer species HPO_4^{2-} and $H_2PO_4^-$ and for NAD^+ were available from literature (Table 1). The parameters for GAP were not available from literature and they could not be determined based on experimental data due to unavailability of pure GAP. Thus, the ePC-SAFT parameters were estimated to be equal to those of 3-phosphoglycerate (3-PG) published elsewhere *(14)*. This assumption might lead to some modeling uncertainty, which can be considered small because 3-PG has a very similar chemical structure compared to GAP (the aldehyde group on the first carbon atom in GAP is replaced by a carboxylate group in 3-PG, but the two other functional groups are the same). Moreover, both, GAP and 3-PG were modeled as species with valence -2, which mainly determines their activity coefficients at very low concentrations present in this work. The parameters for BPG were also not available from literature and had to be estimated, especially also as BPG cannot be purchased commercially. Therefore, the parameters of 3-phosphoglycerate (3-PG) *(14)* and HPO_4^{2-} *(24)* were combined according to a procedure proposed by Do et al. Following this procedure, the segment numbers of 3-PG and HPO_4^{2-} were summed and that of water was subtracted from this in order to calculate that of BPG, see eq. (15).

$$m_{BPG}^{seg} = m_{3\text{-}PG}^{seg} + m_{HPO_4^{2-}}^{seg} - m_{H_2O}^{seg} \quad (15)$$

The segment diameters of 3-PG and HPO_4^{2-} were averaged with a weighing factor w that considers the molecular masses, see eq. (16). w is the ratio of the molecular mass of 3-PG in the molecular mass of BPG (w= $(M_{3\text{-PG}} - M_{OH^-})/M_{BPG}$).

$$\sigma_{BPG} = w \cdot \sigma_{3\text{-}PG} + (1 - w) \cdot \sigma_{HPO_4^{2-}} \quad (16)$$

The dispersion energy of BPG was estimated by the geometric mean of the values of 3-PG and HPO_4^{2-}. The association parameters of BPG $\varepsilon^{A_iB_i}/k_B$ and $\kappa^{A_iB_i}$ were inherited from 3-PG. The parameters of NADH were also determined in this work by fitting to new experimental osmotic coefficients and aqueous densities from literature. The disodium salt of NADH was used which dissociates into two Na^+ and one $NADH^{2-}$ and consequently, the valence 2- was considered for parameter estimation. This is also the valence of NADH under conditions used in this work. Parameters available from literature were used for NAD^+. The following objective function OF in eq. (17) was used for fitting using a Levenberg-Marquardt algorithm for the number of experimental data points NP. Parameters were fitted to densities ρ and osmotic coefficients ϕ.

$$OF = \sum_{k=1}^{NP(\phi)} \left(\phi_k^{ePC-SAFT} - \phi_k^{exp}\right)^2 + \sum_{m=1}^{NP(\rho)} \left(\rho_m^{ePC-SAFT} - \rho_m^{exp}\right)^2 \quad (17)$$

The average absolute deviation (AAD) and the average relative deviation (ARD) of the ePC-SAFT modeled data compared to the experimental data was calculated applying eqs. (18) and (19).

$$AAD = \frac{1}{NP} \sum_{k=1}^{NP} \left| y_k^{ePC-SAFT} - y_k^{exp} \right| \quad (18)$$

$$ARD = \frac{1}{NP} \sum_{k=1}^{NP} \left| 1 - \frac{y_k^{ePC-SAFT}}{y_k^{exp}} \right| \cdot 100\% \quad (19)$$

The resulting pure-component PC-SAFT parameters and the binary interaction parameters estimated in this work, as well as the parameters inherited from literature are listed in Table 1.

Table 1: ePC-SAFT parameters applied in this work with the sources for the respective sets of parameters.

	m_i^{seg}	σ_i	u_i/k_B	N_i^{asso}	$\varepsilon^{A_iB_i}/k_B$	$\kappa^{A_iB_i}$	k_{i,H_2O}	z	source
	-	Å	K	-	K	-	-	-	
NAD^+	25.0875[f]	2.2714[f]	299.04	8+8	3557.3	0.001	-0.074	-	*(28)*
NADH	27.3947	2.7559	380.52	8+8	3711.9	0.001	-0.056	-2	this work
GAP[a]	3.1100	4.6600	322.02	5+5	501.2	0.0001	[b]	-2	*(14)*
BPG	2.9053	2.3452	216.84	5+5	501.2	0.0001	-	-4	this work [c]
water	1.2047	[d]	353.94	1+1	2425.7	0.04509	-	-	*(41)*
HPO_4^{2-}	1	2.1621	146.02	-	-	-	0.25	-2	*(24)*
$H_2PO_4^-$	1	3.6505	95.00	-	-	-	0.25	-1	*(24)*
H_3O^+	1	2.8449	360.00	-	-	-	-0.25	+1	*(24)*
K^+	1	3.3417	200.00	-	-	-	[e]	+1	*(24)*
Mg^{2+}	1	3.1327	1500.00	-	-	-	-0.25	+2	*(24)*
Cl^-	1	2.7560	170.00	-	-	-	-0.25	-1	*(24)*

[a] parameters for GAP were inherited from 3-PG

[b] $k_{GAP,water}$ = 0.0020333 T/K – 0.7063954 *(14)*

[c] parameters determined with a method proposed by HT. Do (see acknowledgement)

[d] σ_{water} = 2.7927 + 10.11 exp(-0.01775 T) – 1.417 exp(-0.01146 T) *(41)*

[e] $k_{K+,water}$ = -0.004012 T/K + 1.3959 *(24)*

[f] typo in the orig. reference from Wangler et al. The values given here have to be used.

Table 2: Binary interaction parameters $k_{i,j}$ between ions used in this work *(24)*.

$k_{cation,anion}$	H_3O^+	K^+	Mg^{2+}
Cl^-	0.654	0.064	0.817
$H_2PO_4^-$	-	0.018	-
HPO_4^{2-}	-	1.000	-
NADH	-	-	-
GAP	-	-	-
BPG	-	-	-

Osmotic coefficients and densities

The five pure-component parameters of NADH and the binary interaction parameter between NADH and water were fitted to osmotic coefficients and densities of the system water and Na_2NADH. This was necessary because the available parameters in literature for NADH did not include the valence of the molecule, which is present under conditions in this work. Thus, using the new set of parameters estimated in this work, yields better results for the prediction of thermodynamic properties such as activity coefficients and osmotic coefficients especially at very low concentrations of NADH in water, see Figure 1. Further, the model is able to better describe

interactions between charged components and ions like Mg^{2+} if the charge of the component is considered in the model parameters. It was assumed that Na_2NADH was fully dissociated in water and the presence of Na^+ was explicitly accounted for in the ePC-SAFT parameter estimation and modeling. The results generated using the new set of parameters from this work show high accuracy regarding densities and osmotic coefficients. Very important is the difference between the modeling from Wangler et al. *(28)* and the modeling from this work at low m_{Na_2NADH} in Figure 1b. These are conditions similar to those used for equilibrium measurements in this work.

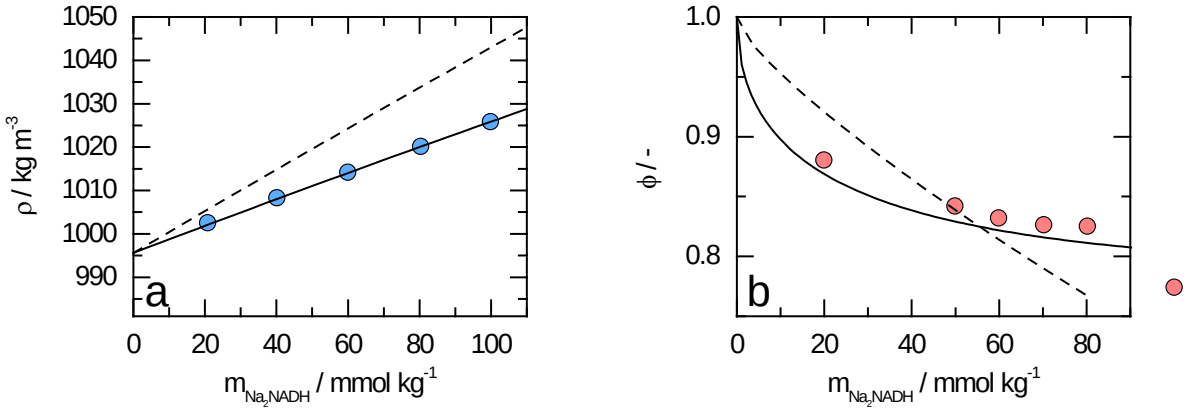

Figure 1: a: Density ρ vs molality of Na_2NADH m_{Na_2NADH} in aqueous solution at 303.15 K and 1 bar. Circles represent experimental data from Wangler et al. *(28)*, solid line represents modeling with ePC-SAFT using parameters from Table 1, dashed line represents modeling with ePC-SAFT using parameters from *(28)* **b:** Osmotic coefficient ϕ vs molality of Na_2NADH m_{Na_2NADH} in aqueous solution at 273.15 K and 1 bar. Circles represent experimental data from this work, solid line represents modeling with ePC-SAFT using parameters from Table 1, dashed line represents modeling with ePC-SAFT using parameters from *(28)*. Please note, that there is a typo in the original source regarding the temperature at which the density measurement was performed (298.15 K) and use the temperature at which the measurement was really performed (303.15 K).

ARD(ϕ) = 1.4%, AAD(ϕ) = 0.01, ARD(ρ) = 0.02%, AAD(ρ) = 0.2 kg m^{-3}, with parameters from this work.

Results

Equilibrium Concentrations and Equilibrium-Molality Ratio

The equilibrium-molality ratio K'_m was calculated from equilibrium concentrations with eq. (6). The equilibrium concentrations were determined with equilibrium measurements that yielded a time-dependent absorbance progression of NADH as shown in Figure 2. When equilibrium was reached, the absorbance of NADH did not change any further and the concentration of NADH was calculated using the respective calibration curve. Furthermore, the equilibrium was validated by adding new substrate and observing again a production of NADH and thus, again an increase of the absorbance. pH measurements were performed yielding proton activity. Thus, the activity coefficient of the proton was predicted from the given proton activity in order to receive the unknown proton molality. This was achieved by applying ePC-SAFT. This procedure yielded values for the equilibrium-molality ratio K'_m of (2.0±0.5)·10^{-7} at $2 \cdot m_{GAP}^{t=0} = m_{NAD^+}^{t=0} =$ 1 mmol kg^{-1}, $m_{P_i}^{t=0} = 80$ mmol kg^{-1}, 298.15 K, pH 7 and 1 bar and (1.8±0.1)·10^{-7} at $m_{GAP}^{t=0} = m_{NAD^+}^{t=0} = 1$ mmol kg^{-1}, $m_{P_i}^{t=0} = 80$ mmol kg^{-1}, 298.15 K, pH 7 and 1 bar.

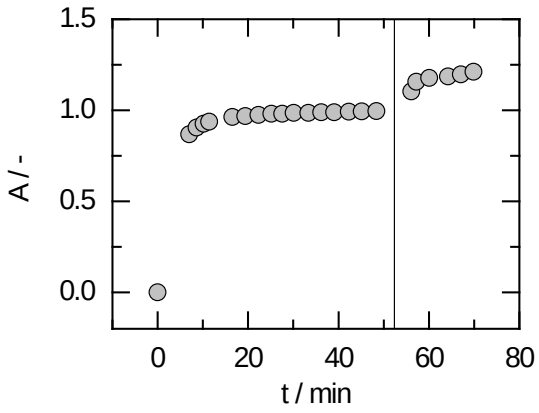

Figure 2: Absorbance A of NADH vs time t. Circles represent measurements, solid line represents addition of new substrate.

Thermodynamic Equilibrium constant and Standard Gibbs Energy of GDH Reaction

The standard Gibbs energy of biochemical reaction $\Delta^R g'^0$ was calculated from the thermodynamic equilibrium constant K'_a with eq. (4). Therefore, the equilibrium-molality ratio K'_m and K'_γ were multiplied. K'_γ was calculated with eq. (7) from activity coefficients of the reactants and products. The equilibrium measurements were performed at 298.15 K and pH 7. The activity coefficients were predicted with ePC-SAFT at the same conditions at which the equilibrium measurements were performed. This means that all substances, which were present in the multi-component reaction medium in the equilibrium measurements except the enzyme, were considered explicitly. This includes the substrates GAP, NAD^+ and P_i, the products BPG, NADH and H_3O^+, as well as the ions Mg^{2+}, Cl^- and K^+. The pure-component parameters and binary interaction parameters, which are required for these predictions, are listed in Table 1 and Table 2, respectively. The resulting K'_m, K'_γ and K'_a are shown in Figure 3.

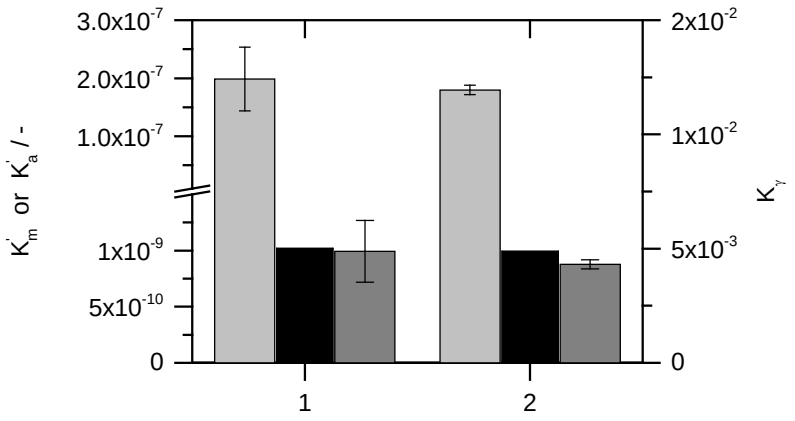

315

316 **Figure 3:** Equilibrium-molality ratio K'_m (light gray bars), activity-coefficient ratio K'_γ (black bars)

317 and thermodynamic equilibrium constant K'_a (dark gray bars) for $2 \cdot m_{GAP}^{t=0} = m_{NAD^+}^{t=0} =$

318 1 mmol kg^{-1} (1) and $m_{GAP}^{t=0} = m_{NAD^+}^{t=0} = 1$ mmol kg^{-1} (2) at 298.15 K, $m_{P_i}^{t=0} = 80$ mmol kg^{-1}, pH 7

319 and 1 bar.

320 The calculations yield a thermodynamic equilibrium constant K'_a(298.15 K) = (0.9±0.2)·10^{-9}.

321 $\Delta^R g'^0$(298.15 K) calculated from this value with eq. (4) is 51.5±0.4 kJ mol^{-1}.

Table 3: Equilibrium-molality ratio K'_m calculated according to eq. (6) at experimental conditions (columns 1-9 and 1 bar, $m^{eq}_{H^+}$ was calculated with ePC-SAFT), activity coefficient ratio K'_γ, equilibrium constant K'_a and standard Gibbs energy of reaction $\Delta^R g'^0$.

T	pH	m^{eq}_{NAD+}	m^{eq}_{NADH}	m^{eq}_{GAP}	m^{eq}_{BPG}	$m^{eq}_{P_i}$	$m^{eq}_{H^+} \cdot 10^4$	$m_{Mg^{2+}}$	$K'_m \cdot 10^7$	$K'_\gamma \cdot 10^3$	$K'_a \cdot 10^9$	$\Delta^R g'^0$
K	-	mmol kg^{-1}	mmol kg^{-1}	mmol kg^{-1}	mmol kg^{-1}	mmol kg^{-1}	mmol kg^{-1}	mmol kg^{-1}	-	-	-	kJ mol^{-1}
298.15	7.0	0.79±0.02	0.17±0.01	0.32±0.03	0.17±0.01	79.8±0.1	1.3	0	2.0±0.5	5.0	1.0±0.3	51.4±0.7
298.15	7.0	0.69±0.01	0.23±0.01	0.74±0.02	0.23±0.01	80.3±0.2	1.3	0	1.8±0.1	4.9	0.9±0.1	51.7±0.1
305.15	7.0	0.83±0.01	0.19±0.01	0.31±0.02	0.19±0.01	80.6±0.1	1.4	0	2.5±0.3	4.7	1.2±0.1	52.2±0.3
310.15	7.0	0.78±0.01	0.18±0.01	0.30±0.02	0.18±0.01	81.6±0.1	1.4	0	2.5±0.2	4.4	1.1±0.1	53.2±0.2
310.15	7.0	0.69±0.02	0.27±0.01	0.76±0.04	0.27±0.01	80.5±0.4	1.3	0	2.4±0.4	4.3	1.0±0.2	53.4±0.5
298.15	7.0	0.63±0.01	0.28±0.01	0.70±0.02	0.28±0.01	78.6±0.2	1.4	11.0	3.2±0.1	3.3	1.1±0.1	51.2±0.1
298.15	7.0	0.57±0.01	0.32±0.01	0.62±0.03	0.32±0.01	76.1±0.2	1.3	20.1	4.8±0.6	2.5	1.2±0.1	50.9±0.3

Influence of pH and Mg^{2+} on reaction equilibrium

To determine the influence of the pH value on the GDH reaction, the equilibrium-molality ratio K'_m was determined at different pH values and was converted to the equilibrium constant K'_a using activity coefficients and eq. (5). The dependence of K'_m of the GDH reaction on pH is shown in Figure 4 and Table 4. An increase of pH yields a significant increase of K'_m.

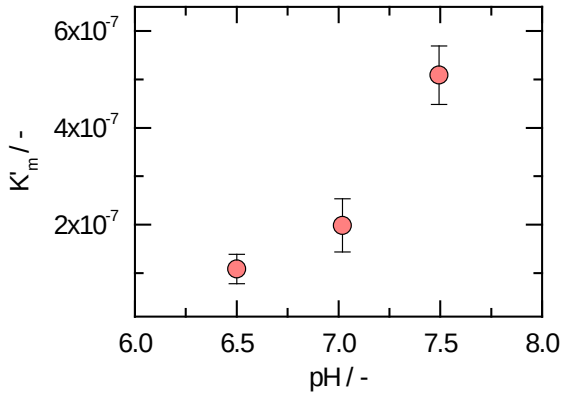

Figure 4: Equilibrium-molality ratio K'_m of biochemical reaction vs pH at 298.15 K and 1 bar. Circles represent K'_m values from this work.

Table 4: Equilibrium-molality ratio K'_m calculated according to eq. (6) at experimental conditions (columns 1-8 and 1 bar, $m^{eq}_{H^+}$ was calculated with ePC-SAFT).

T	pH	$m^{eq}_{NAD^+}$	m^{eq}_{NADH}	m^{eq}_{GAP}	m^{eq}_{BPG}	$m^{eq}_{P_i}$	$m^{eq}_{H^+} \cdot 10^4$	$K'_m \cdot 10^7$
K	-	mmol kg^{-1}	mmol kg^{-1}	mmol kg^{-1}	mmol kg^{-1}	mmol kg^{-1}	mmol kg^{-1}	-
298.15	6.5	0.84±0.01	0.08±0.01	0.41±0.02	0.08±0.01	80.1±0.1	4.3	1.1±0.3
298.15	7.0	0.79±0.02	0.17±0.01	0.32±0.03	0.17±0.01	79.8±0.1	1.3	2.0±0.5
298.15	7.5	0.63±0.01	0.31±0.01	0.18±0.02	0.31±0.01	79.5±0.1	0.5	5.1±0.6

Many biochemical reactions are not only dependent on pH, but also somehow dependent on Mg^{2+}. This might be due to the enzyme requiring Mg^{2+} as a cofactor in order to catalyze a specific reaction, or due to the formation of Mg^{2+}-substrate-complexes, which represent the reacting species *(11,14,42)*. In both cases, the lack of Mg^{2+} in the reaction solution would result in no product formation, which is not the case for this reaction. However, Mg^{2+} may also influence a reaction in the same way as pH (i.e. the amount of H^{+}-ions in solution) does: by forming Mg^{2+}-substrate complexes, the molality of the reacting species is reduced, which shifts the equilibrium position of the biochemical reaction for different Mg^{2+} molalities. Another way for Mg^{2+} to influence the reaction is by its influence on the activity coefficients of the reactants and products of the reaction and thereby, on the equilibrium of the reaction. The latter assumes that complexes or intermediates including Mg^{2+} are not formed.

To determine the influence of Mg^{2+} on the equilibrium of the GDH reaction K'_m was measured at different magnesium chloride molalities. This is shown in Figure 5a: K'_m increases from $1.8 \cdot 10^{-7}$ to $4.8 \cdot 10^{-7}$ with increasing Mg^{2+} molality. Values of 11 and 20 mmol kg^{-1} total Mg^{2+} correspond to 1 and 2 mmol kg^{-1} free Mg^{2+}, respectively, which was calculated using pK_A values from Vojinovic and von Stockar *(8)* and Schneider et al. *(43)*, see Supporting Information. Contrarily, Figure 5c shows that K'_a does not change with varying $MgCl_2$ molality but is a constant number. The reason for this behavior is the activity coefficient-ratio, which is decreasing with increasing Mg^{2+} molality, see Figure 5b. The fact that Mg^{2+} influences the activity coefficients in the shown way proves that complexes are not formed, and that the reason behind the influence is the interaction between Mg^{2+} and the reacting substances. Especially the interaction between BPG and Mg^{2+} is strong; Figure 6 shows the activity coefficients of the reactants and products. The activity coefficient of BPG at 20 mmol kg^{-1} Mg^{2+} is 48% smaller than at the Mg^{2+}-free solution, while the difference for all other reactants and products is less than 8%. Thus, the attraction between Mg^{2+} and BPG causes the

influence of Mg^{2+} on the reaction equilibrium. This interaction is comparatively strong, but it does not cause complex formation; the latter would cause results much different from these observations.

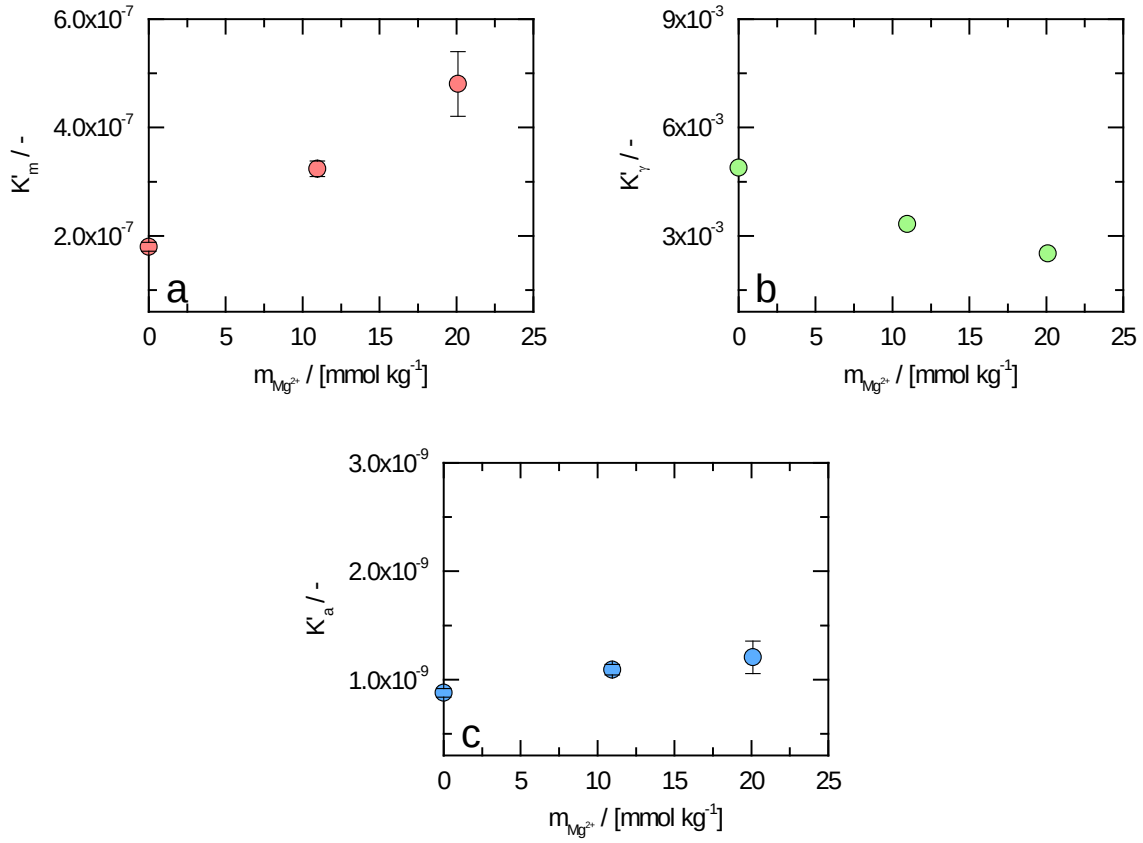

Figure 5: **a:** Equilibrium-molality ratio of biochemical reaction K'_m vs Mg^{2+} molality $m_{Mg^{2+}}$ at 298.15 K and 1 bar. Circles represent K'_m values from this work. **b:** Activity-coefficient ratio of biochemical reaction K'_γ vs Mg^{2+} molality $m_{Mg^{2+}}$ at 298.15 K and 1 bar. Circles represent K'_γ values from this work predicted with ePC-SAFT. **c:** Equilibrium constant of biochemical reaction K'_a vs Mg^{2+} molality $m_{Mg^{2+}}$ at 298.15 K and 1 bar. Circles represent K'_a values from this work. $m_{Mg^{2+}}$ = 11 mmol kg^{-1} corresponds to $m^{free}_{Mg^{2+}}$ = 1 mmol kg^{-1} and $m_{Mg^{2+}}$ = 20 mmol kg^{-1} corresponds to $m^{free}_{Mg^{2+}}$ = 2 mmol kg^{-1}.

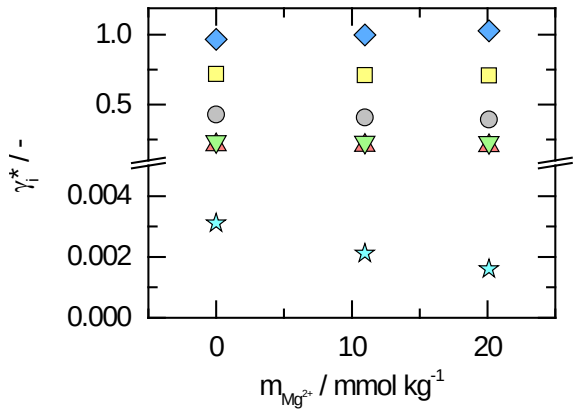

372

373 **Figure 6:** Rational activity coefficients of reactants and products γ_i^* vs Mg^{2+} molality $m_{Mg^{2+}}$ at
374 298.15 K and 1 bar. Diamonds: NAD^+, squares: H^+, triangles with laces down: GAP, triangles with
375 laces up: NADH, circles: P_i, and stars: BPG.

376 **Standard Enthalpy of GDH Reaction**

377 To determine the standard enthalpy of reaction $\Delta^R h'^0$, equilibrium measurements were performed
378 and the van 't Hoff equation was applied (see eq. (9)). This is only consistent using thermodynamic
379 equilibrium constants (K'_a), which were determined at 298.15 K, 305.15 K and 310.15 K. $ln(K'_a)$
380 was plotted against $1/T$ (van 't Hoff plot) as shown in Figure 7.

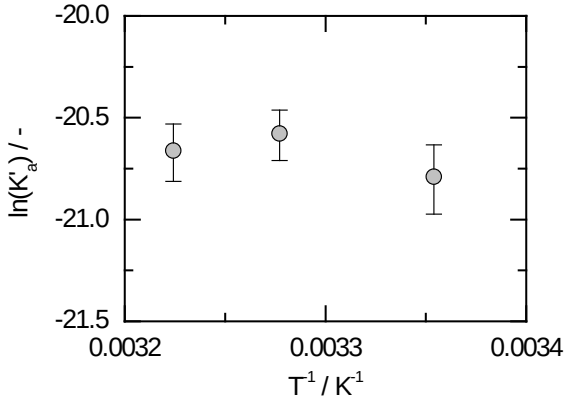

381

382 **Figure 7:** Natural logarithm of equilibrium constant of biochemical reaction K'_a vs inverse
383 temperature at pH 7 and 1 bar.

It can be observed that the $ln(K'_a)$ values do not differ from each other within the error bars between 298.15 K and 310.15 K. Applying the van 't Hoff equation yields $\Delta^R h'^0$ = 9±16 kJ mol^{-1}. This high uncertainty stems from the error estimation of the single K'_a values and are thus caused by the equilibrium experiments. For the considered reaction, the procedure seems rather less appropriate to determine a precise value for $\Delta^R h'^0$. Thus, we determined $\Delta^R h'^{0,obs}$ with calorimetric measurements. With this procedure we measured a heat released during the GDH reaction of Q = 720±13 µJ. We calculated $\Delta^R h'^{0,obs}$ = 4.6±0.1 kJ mol^{-1} from Q with eq. (20).

$$\Delta^R h'^{0,obs} = \frac{Q}{n^{eq}_{NADH}} = \frac{Q}{m^{eq}_{NADH} \cdot m_{cell}} \tag{20}$$

Therefore, we determined the moles of NADH produced during the reaction from the mass within the measurement cell m_{cell} and the molality of NADH at equilibrium m^{eq}_{NADH} using ePC-SAFT. We determined the equilibrium-molality ratio K'_m that yields m^{eq}_{NADH} from the known K'_a at 310.15 K (found in this work) and the known substrate molalities by iteratively changing K'_m and predicting the corresponding K'_γ until K'_a reached the known value. Due to the extremely low substrate molalities chosen for the calorimetric measurements it might be reasonable to assume that the enthalpy of reaction $\Delta^R h'^{0,obs}$ determined here is close to the standard enthalpy of reaction $\Delta^R h'^0$. Indeed, we found from the ePC-SAFT predictions that the activity-coefficient ratio K'_γ is constant at the conditions applied in the ITC (400 mmol kg^{-1} phosphate buffer, starting concentration of NAD^+ 5 mmol kg^{-1} and GAP 0.9 mmol kg^{-1}) for the two temperatures 298.15 K and 310.15 K. Both, the calorimetric measurements and the equilibrium measurements yield a slightly endothermic value for $\Delta^R h'^0$, supporting that the GDH reaction is indeed slightly endothermic.

Discussion

In this work, the standard Gibbs energy of biochemical GDH reaction $\Delta^R g'^0$ was calculated applying eq. (4) using the thermodynamic equilibrium constant K'_a, which finally yields an activity-based value. This value is independent of any concentrations (substrates or products, other substances present in the reaction medium). $\Delta^R g'^0$ and K'_a from this work do only depend on temperature, and pressure (not investigated in this work). On the contrary, values available in literature and discussed in the following are concentration-based values. Further, the concentration of protons H^+ was not considered for the calculation of equilibrium-molality ratio or standard Gibbs energies of reaction. Thus, values from literature have to be transformed into activity-based values and protons have to be included in the calculation. To predict activity coefficients, which are required to calculate K'_a, the reaction medium composition and reaction conditions have to be known. The literature K'_m values are thus only valid at the conditions they were measured, but not at any other conditions. Hence, those values available in literature were chosen for comparison, which were measured at reaction conditions similar to those applied in this work, see Table 5. Meyerhof and Oesper measured at different conditions compared to the present work (lower $m^{init}_{NAD^+}$, but at similar m^{init}_{GAP} and $m^{init}_{P_i}$ compared to the present work). They measured at pH 7 and 295.15 K and added glutathionine for enzyme stabilization, which is not considered in the following calculations. They give a K'_m/m_{H^+} of 0.68 kg mol^{-1}. Prediction of m_{H^+} with ePC-SAFT yields $K'_m = 0.9 \cdot 10^{-7}$. Further, prediction of the activity coefficients of the substrates and products yields $K'_a = 1.1 \cdot 10^{-9}$. Cori et al. *(19)* measured also at different conditions (compared to the present work: lower $m^{init}_{NAD^+}$, higher m^{init}_{GAP} and similar $m^{init}_{P_i}$ at pH 7.1 and unknown temperature (for all calculations 298.15 K was assumed)). They give a K'_m/m_{H^+} of about 0.66±0.01 kg mol^{-1}. Prediction of m_{H^+} with ePC-SAFT yields $K'_m = 0.75 \cdot 10^{-7} \pm 0.05 \cdot 10^{-7}$. Further, prediction of the

activity coefficients of the substrates and products yields an average $K'_a = 0.7 \cdot 10^{-9}$. Cornell et al. *(20)* measured at several reaction conditions (see Table 5) at 6.9 < pH < 7.1 at 311.15 K. They specified a value of $K'_m \cdot \gamma_{H^+}^{*,m} = 0.51 \cdot 10^{-7} \pm 0.02 \cdot 10^{-7}$, for which they used the proton activity from a pH measurement for calculation. Prediction of m_{H^+} with ePC-SAFT yields $K'_m = 0.69 \cdot 10^{-7} \pm 0.03 \cdot 10^{-7}$. Further, prediction of the activity coefficients of the substrates and products yields an average value of $K'_a = 0.8 \cdot 10^{-9}$. The measurements of Cornell et al. were performed under presence of $MgCl_2$, which was considered for the ePC-SAFT predictions. Further, they added KCl in order to adjust ionic strength to 0.25 M. This could not be considered for the ePC-SAFT predictions in this work as the exact amount of KCl, which was added is unknown. In an own attempt to determine an activity-based value, Cornell et al. plotted $log(K'_m)$ versus the square root of ionic strength and extrapolated to zero ionic strength, which yielded a value of $0.1 \cdot 10^{-7}$. It remains unclear if all charged components such as substrates and products were included in the calculation of the ionic strength. However, interactions involving the substrates and products were not accounted for in their work. This explains the difference between their value ($0.1 \cdot 10^{-7}$) and the value determined in the present work ($1 \cdot 10^{-9}$). For further comparison at isothermal conditions, the value of $\Delta^R h'^0(\text{pH } 7) = 4.6$ kJ mol^{-1} was used to convert the literature K'_m values to 298.15 K (Table 5; Figure 8). Further, the respective pH values of the literature sources (6.9<pH<7.1) were used to calculate K'_m and K'_a values in Table 5 using eqs. (5) and (6). As shown in Figure 8, the equilibrium-molality ratios K'_m measured from Meyerhof and Oesper, Cori et al. and Cornell et al. are all significantly lower than those measured in this work. However, including activity coefficients to the calculation yields very good agreement between the activity-based equilibrium constants of the mentioned authors and this work. Deviations between the different K'_a values determined might result from the presence of components in the reaction medium, which have not

been considered in the calculation (such as glutathionine for Meyerhof and Oesper or others that might be even unknown). Moreover, only Cornell et al. estimated the errors of their data, which makes a comparison with the data from the other authors difficult.

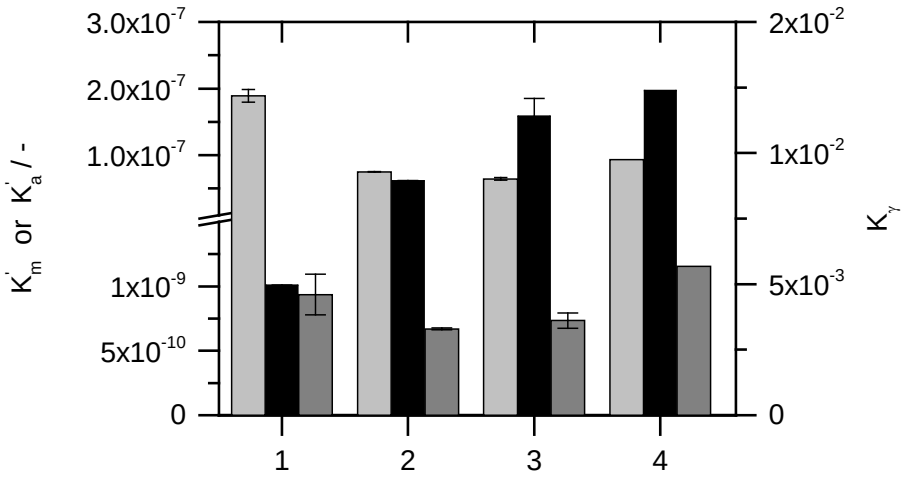

Figure 8: Equilibrium-molality ratio K'_m (light gray bars), activity-coefficient ratio K'_γ (black bars) and thermodynamic equilibrium constant K'_a (dark gray bars), see Table 5 for reaction conditions at 298.15 K or converted to 298.15 K. 1: This work, 2: based on values from Cori et al. *(19)*, 3: based on values from Cornell et al. *(20)*, 4: based on values from Meyerhof and Oesper *(18)*. Error bars at literature values represent standard deviation resulting from separate measurements.

Table 5: Equilibrium-molality ratio K'_m calculated according to eq. (6) (at conditions given in columns 2-5) using ePC-SAFT to predict $m_{H^+}^{eq}$, activity-coefficient ratio of biochemical reaction K'_γ and equilibrium constant of biochemical reaction K'_a. K'_m and K'_a were converted from original temperatures $T^{original}$ to 298.15 K using $\Delta^R h'^0(\text{pH } 7) = 4.6$ kJ mol^{-1} determined with ITC measurements in this work.

$T^{original}$	pH	$m_{NAD^+}^{init}$	m_{GAP}^{init}	$m_{P_i}^{init}$	K'_m $\cdot 10^7$	K'_γ $\cdot 10^2$	K'_a $\cdot 10^9$	source
K	-	mmol kg^{-1}	mmol kg^{-1}	mmol kg^{-1}	-	-	-	
298.15	7.0	1.0	0.5	80.0	2.0±0.5	0.5	1.0±0.3	this work
298.15	7.0	0.9	1.0	80.5	1.8±0.1	0.5	0.9±0.1	this work
295.15	7.0	0.2	1.1	82.5	0.9	1.2	1.2	*(18)*
[a]	7.1	0.1	1.4	82.8	0.8	0.9	0.7	*(19)*
[a]	7.1	0.1	1.4	82.8	0.7	0.9	0.7	*(19)*
311.15	7.1	1.2	0.3	79.3	0.7	1.1	0.7	*(20)*
311.15	7.1	0.7	0.2	80.6	0.6	1.1	0.7	*(20)*
311.15	7.1	0.7	0.2	80.6	0.6	1.1	0.7	*(20)*
311.15	6.9	0.5	0.2	84.2	0.7	1.2	0.8	*(20)*
311.15	6.9	1.0	0.2	83.8	0.6	1.2	0.8	*(20)*
311.15	6.9	0.5	0.4	84.0	0.7	1.2	0.8	*(20)*

[a] temperature not given, calculations performed at 298.15 K

The comparison of different literature values shows that concentration-based K'_m values and for this reason concentration-based observed standard Gibbs energies of reaction $\Delta^R g'^{0,obs}$ differ significantly from each other. This becomes even clearer when influences of single changes of the reaction medium are investigated, such as the influence of Mg^{2+} on the reaction. As shown in Figure 5, Mg^{2+} strongly influences K'_m values by more than 100% even at low Mg^{2+} molality. It is thus a consequence that these different conditions also cause different $\Delta^R g'^{0,obs}$ values. Thus, it is essential to determine K'_a and $\Delta^R g'^0$ in order to get thermodynamically correct values that do not depend on the composition of the reaction medium. This illustrates the usefulness of a suitable thermodynamic model such as ePC-SAFT, which allows considering the influence of the composition of the reaction medium (e.g., Mg^{2+}) on the reaction equilibrium. Further, K'_m showed a pH dependence from equilibrium data of this work, at least at a pH value between 6.5 and 7.5, see Figure 4.

The thermodynamic equilibrium constant K'_a showed a temperature dependence in the equilibrium experiments performed in this work in the temperature range of 298.15 K to 310.15 K yielding a standard reaction enthalpy $\Delta^R h'^0$ of 9±16 kJ mol^{-1}. Using titration calorimetry a more accurate value of $\Delta^R h'^0$= 4.6±0.1 kJ mol^{-1} was obtained. Meyerhof and Oesper *(18)* stated that there is no temperature dependence of the reaction in the temperature range of 295.15 K to 305.15 K. In the textbook of Scott *(44)*, a value of -2.9 kJ mol^{-1} is listed, but it remains unclear where this value originates from and how it was measured or calculated. Thus, we recommend using a value of $\Delta^R h'^0$(pH 7) = 4.6±0.1 kJ mol^{-1} for future works.

Based on $\Delta^R g'^0$ and $\Delta^R h'^0$ determined in this work, it is possible to determine at which conditions the GDH reaction is feasible in a cell. Therefore, reaction conditions, like concentrations of the metabolites in a cell, are required in combination with an approach like that described in this work

applying ePC-SAFT in order to determine the activity coefficients. This will show how the GDH reaction is influenced by the conditions within a cell, which is important for the glycolytic pathway as a whole because the GDH is one of the most important reactions regarding its feasibility.

Conclusion

The thermodynamic equilibrium constant K'_a and the standard Gibbs energy of reaction $\Delta^R g'^0$ of the GDH reaction were determined in this work based on equilibrium measurements and activity coefficients predicted from ePC-SAFT. A value of K'_a(298.15 K) = (0.9±0.2)·10^{-9} was determined, which yields $\Delta^R g'^0$(298.15 K) = 51.5±0.4 kJ mol^{-1}. Both values are constant values at 298.15 K and do not depend on other influences of the reaction medium such as concentrations of substrates, products, or Mg^{2+}. The K'_a value from this work is in good agreement with those of Cori et al. *(19)* and Cornell et al. *(20)*, which were calculated from their concentration-dependent K'_m values and own ePC-SAFT modeling. The standard enthalpy of GDH reaction was determined from experiments performed at different temperatures of 298.15 K, 305.15 K and 310.15 K together with activity coefficients from ePC-SAFT to be $\Delta^R h'^0$ = 9±16 kJ mol^{-1}. Titration calorimetry experiments performed in the present work yielded a more accurate value of 4.6±0.1 kJ mol^{-1}, which is recommended for future works. Influences of the pH value and Mg^{2+} on the reaction equilibrium were also investigated. Experiments at pH values of 6.5 and 7.5 showed that pH has an influence on the reaction equilibrium, especially at pH>7. Values of K'_m(298.15 K, pH 6.5) = (1.1±0.3)·10^{-7} and K'_m(298.15 K, pH 7.5) = (5.1±0.6)·10^{-7} were determined. Experiments at Mg^{2+} molalities up to 20 mmol kg^{-1} showed that K'_m significantly increases with increasing Mg^{2+} molality. The reason for this was found to be the activity coefficients of the products BGP, which

were significantly decreased by Mg^{2+}. The ePC-SAFT parameters were taken from literature, except those for NADH and BPG. Parameters for NADH were fitted to aqueous densities from literature and own experimental osmotic coefficients, parameters for BPG were determined based on a procedure provided by our colleague HT Do. The standard Gibbs energy of reaction $\Delta^R g'^0$ can be used in future works to determine the Gibbs energy of reaction $\Delta^R g'$, which finally allows to determine the feasibility of the GDH reaction at different reaction conditions.

Accession ID for the enzyme glyceraldehyde 3-phosphate dehydrogenase

Glyceraldehyde 3-phosphate dehydrogenase was used from rabbit muscle (UniProtKB - P46406).

Acknowledgement

This work was supported by the German Science Foundation (DFG) grant No. HE7165/5-1, MA3746/6-1 and SA700/20-1 (Leibniz award to G. Sadowski). The authors thank Hoang Tam Do for providing a method, which allows determining unknown ePC-SAFT parameters of a substance based on known parameters of similar substances.

Supporting Information

Supporting information is available online.

References

1. ter Kuile, B. H., and Westerhoff, H. V. (2001) Transcriptome meets metabolome: hierarchical and metabolic regulation of the glycolytic pathway, *FEBS Lett. 500,* 169–171.

2. Bar-Even, A., Flamholz, A., Noor, E., and Milo, R. (2012) Rethinking glycolysis: on the biochemical logic of metabolic pathways, *Nat. Chem. Biol. 8,* 509–517.

3. Selig, M., Xavier, K. B., Santos, H., and Schönheit, P. (1997) Comparative analysis of Embden-Meyerhof and Entner-Doudoroff glycolytic pathways in hyperthermophilic archaea and the bacterium Thermotoga, *Arch. Microbiol. 167,* 217–232.

4. Turner, J. F., and Turner, D. H. (1980) The Regulation of Glycolysis and the Pentose Phosphate Pathway, in *Metabolism and Respiration*, pp 279–316, Elsevier.

5. Churchill, T. A., Green, C. J., and Fuller, B. J. (1995) Stimulation of glycolysis by histidine buffers in mammalian liver during cold hypoxia, *Arch. Biochem. Biophys. 320,* 43–50.

6. Maitra, P. K., and Lobo, Z. (1978) Reversal of glycolysis in yeast, *Arch. Biochem. Biophys. 185*, 535–543.

7. Maskow, T., and von Stockar, U. (2005) How reliable are thermodynamic feasibility statements of biochemical pathways?, *Biotechnol. Bioeng. 92,* 223–230.

8. Vojinovic, V., and von Stockar, U. (2009) Influence of uncertainties in pH, pMg, activity coefficients, metabolite concentrations, and other factors on the analysis of the thermodynamic feasibility of metabolic pathways, *Biotechnol. Bioeng. 103,* 780–795.

9. Burton, K., and Krebs, H. A. (1953) The free-energy changes associated with the individual steps of the tricarboxylic acid cycle, glycolysis and alcoholic fermentation and with the hydrolysis of the pyrophosphate groups of adenosinetriphosphate, *Biochem. J. 54*, 94–107.

10. Mavrovouniotis, M. L. (1993) Identification of Localized and Distributed Bottlenecks in Metabolic Pathways, *Proc. Int. Conf. Intell. Syst. Mol. Biol. 1*, 275–283.

11. Meurer, F., Bobrownik, M., Sadowski, G., and Held, C. (2016) Standard Gibbs Energy of Metabolic Reactions. I. Hexokinase Reaction, *Biochemistry 55,* 5665–5674.

12. Meurer, F., Do, H. T., Sadowski, G., and Held, C. (2017) Standard Gibbs energy of metabolic reactions. II. Glucose-6-phosphatase reaction and ATP hydrolysis, *Biophys. Chem. 223,* 30–38.

13. Hoffmann, P., Held, C., Maskow, T., and Sadowski, G. (2014) A thermodynamic investigation of the glucose-6-phosphate isomerization, *Biophys. Chem. 195,* 22–31.

14. Wangler, A., Schmidt, C., Sadowski, G., and Held, C. (2018) Standard Gibbs Energy of Metabolic Reactions. III The 3-Phosphoglycerate Kinase Reaction, *ACS Omega 3,* 1783–1790.

15. Gao, M., Held, C., Patra, S., Arns, L., Sadowski, G., and Winter, R. (2017) Crowders and Cosolvents-Major Contributors to the Cellular Milieu and Efficient Means to Counteract Environmental Stresses, *Chemphyschem 18,* 2951–2972.

16. Greinert, T., Baumhove, K., Sadowski, G., and Held, C. (2020) Standard Gibbs energy of metabolic reactions: IV. Triosephosphate isomerase reaction, *Biophys. Chem. 258,* 106330.

17. Greinert, T., Vogel, K., Seifert, A. I., Siewert, R., Andreeva, I. V., Verevkin, S. P., Maskow, T., Sadowski, G., and Held, C. (2020) Standard Gibbs energy of metabolic reactions: V. enolase reaction, *BBA-Proteins Proteom. 1868,* 140365.

18. Meyerhof, O., and Oesper, P. (1947) The mechanism of the oxidative reaction in fermentation, *J. Biol. Chem. 170,* 1–22.

19. Cori, C. F., Velick, S. F., and Cori, G. T. (1950) The combination of diphosphopyridine nucleotide with glyceraldehyde phosphate dehydrogenase, *Biochim. Biophys. Acta 4,* 160–169.

20. Cornell, N. W., Leadbetter, M., and Veech, R. L. (1979) Effects of Free Magnesium Concentration and Ionic Strength on Equilibrium Constants for the Glyceraldehyde Phosphate Dehydrogenase and Phosphoglycerate Kinase Reactions, *J. Biol. Chem. 254,* 6522–6527.

21. Stryer, L. (1988) Biochemistry. 3rd ed., Freeman, New York, NY.

22. Alberty, R. A. (1993) Thermodynamics of reactions of nicotinamide adenine dinucleotide and nicotinamide adenine dinucleotide phosphate, *Arch. Biochem. Biophys. 307,* 8–14.

23. Alberty, R. A. (1998) Calculation of standard transformed Gibbs energies and standard transformed enthalpies of biochemical reactants, *Arch. Biochem. Biophys. 353,* 116–130.

24. Held, C., Reschke, T., Mohammad, S., Luza, A., and Sadowski, G. (2014) ePC-SAFT revised, *Chem. Eng. Res. Des. 92,* 2884–2897.

25. Gross, J., and Sadowski, G. (2001) Perturbed-Chain SAFT: An Equation of State Based on a Perturbation Theory for Chain Molecules, *Ind. Eng. Chem. Res. 40,* 1244–1260.

26. Held, C., and Sadowski, G. (2016) Thermodynamics of Bioreactions, *Annu. Rev. Chem. Biomol. Eng. 7,* 395–414.

27. Voges, M., Schmidt, F., Wolff, D., Sadowski, G., and Held, C. (2016) Thermodynamics of the alanine aminotransferase reaction, *Fluid Phase Equilibr. 422,* 87–98.

28. Wangler, A., Loll, R., Greinert, T., Sadowski, G., and Held, C. (2019) Predicting the high concentration co-solvent influence on the reaction equilibria of the ADH-catalyzed reduction of acetophenone, *J. Chem. Thermodyn. 128,* 275–282.

29. Voges, M., Abu, R., Gundersen, M. T., Held, C., Woodley, J. M., and Sadowski, G. (2017) Reaction Equilibrium of the ω-Transamination of (S)-Phenylethylamine: Experiments and ePC-SAFT Modeling, *Org. Process Res. Dev. 21,* 976–986.

30. Voges, M., Fischer, F., Neuhaus, M., Sadowski, G., and Held, C. (2017) Measuring and Predicting Thermodynamic Limitation of an Alcohol Dehydrogenase Reaction, *Ind. Eng. Chem. Res. 56,* 5535–5546.

31. Voges, M., Fischer, C., Wolff, D., and Held, C. (2017) Influence of Natural Solutes and Ionic Liquids on the Yield of Enzyme-Catalyzed Reactions: Measurements and Predictions, *Org. Process Res. Dev. 21,* 1059–1068.

32. Voges, M., Prikhodko, I. V., Prill, S., Hübner, M., Sadowski, G., and Held, C. (2017) Influence of pH Value and Ionic Liquids on the Solubility of l -Alanine and l -Glutamic Acid in Aqueous Solutions at 30 °C, *J. Chem. Eng. Data 62,* 52–61.

33. Voges, M., Herhut, M., Held, C., and Brandenbusch, C. (2018) Light-scattering data of protein and polymer solutions: A new approach for model validation and parameter estimation, *Fluid Phase Equilibr. 465,* 65–72.

34. Wangler, A., Sieder, G., Ingram, T., Heilig, M., and Held, C. (2018) Prediction of CO2 and H2S solubility and enthalpy of absorption in reacting N-methyldiethanolamine /water systems with ePC-SAFT, *Fluid Phase Equilibr. 461,* 15–27.

35. Wangler, A., Canales, R., Held, C., Luong, T. Q., Winter, R., Zaitsau, D. H., Verevkin, S. P., and Sadowski, G. (2018) Co-solvent effects on reaction rate and reaction equilibrium of an enzymatic peptide hydrolysis, *Physical chemistry chemical physics : PCCP 20,* 11317–11326.

36. Wangler, A., Böttcher, D., Hüser, A., Sadowski, G., and Held, C. (2018) Prediction and Experimental Validation of Co-Solvent Influence on Michaelis Constants: A Thermodynamic Activity-Based Approach, *Chemistry (Weinheim an der Bergstrasse, Germany) 24,* 16418–16425.

623 37. Wangler, A., Hüser, A., Sadowski, G., and Held, C. (2019) Simultaneous Prediction of
624 Cosolvent Influence on Reaction Equilibrium and Michaelis Constants of Enzyme-Catalyzed
625 Ketone Reductions, *ACS Omega 4,* 6264–6272.

626 38. Buck, R. P., Rondinini, S., Covington, A. K., Baucke, F. G. K., Brett, C. M. A., Camoes, M.
627 F., Milton, M. J. T., Mussini, T., Naumann, R., Pratt, K. W., Spitzer, P., and Wilson, G. S. (2002)
628 Measurement of pH. Definition, standards, and procedures (IUPAC Recommendations 2002),
629 *Pure Appl. Chem. 74*, 2169–2200.

630 39. Cameretti, L. F., Sadowski, G., and Mollerup, J. M. (2005) Modeling of Aqueous Electrolyte
631 Solutions with Perturbed-Chain Statistical Associated Fluid Theory, *Ind. Eng. Chem. Res. 44,*
632 3355–3362.

633 40. Bülow, M., Ji, X., and Held, C. (2019) Incorporating a concentration-dependent dielectric
634 constant into ePC-SAFT. An application to binary mixtures containing ionic liquids, *Fluid Phase*
635 *Equilibr. 492,* 26–33.

636 41. Cameretti, L. F., and Sadowski, G. (2008) Modeling of aqueous amino acid and polypeptide
637 solutions with PC-SAFT, *Chemical Engineering and Processing: Process Intensification 47,*
638 1018–1025.

639 42. Cowan, J. A. (2002) Structural and catalytic chemistry of magnesium-dependent enzymes,
640 *BioMetals 15,* 225–235.

641 43. Schneider, I. C., Rhamy, P. J., Fink-Winter, R. J., and Reilly, P. J. (1999) High-performance
642 anion-exchange chromatography of sugar and glycerol phosphates on quaternary ammonium
643 resins, *Carbohyd. Res. 322,* 128–134.

644 44. Scott, C. B. (2008) A Primer for the Exercise and Nutrition Sciences. Thermodynamics,
645 Bioenergetics, Metabolism. 1st ed., Humana Press, s.l.

646

647 **Graphical Abstract**

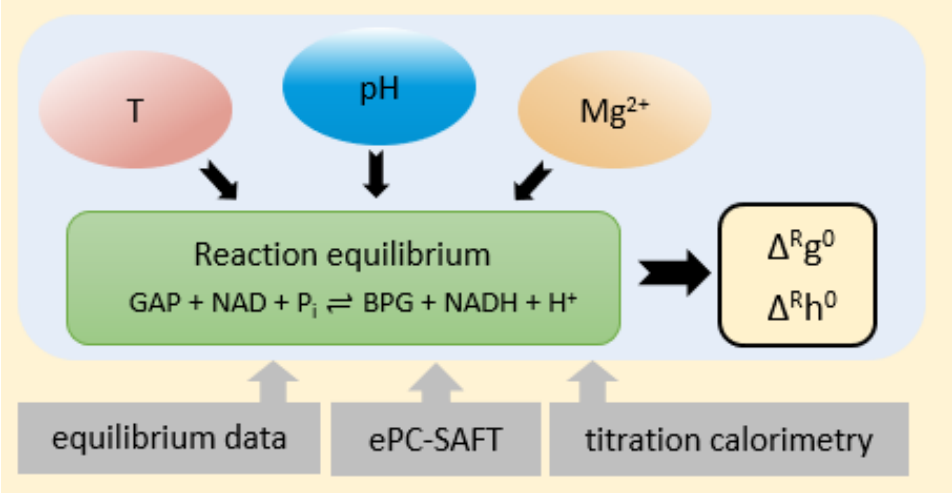

648

649 For Table of Contents Only